

Received October 14, 2020, accepted October 27, 2020, date of publication November 4, 2020, date of current version November 20, 2020.

Digital Object Identifier 10.1109/ACCESS.2020.3035959

UAV and SWIPT Assisted Disaster Aware Clustering and Association

ALI HASSAN¹, RIZWAN AHMAD¹, (Member, IEEE), WAQAS AHMED², (Member, IEEE), MAURIZIO MAGARINI³, (Member, IEEE), AND MUHAMMAD MAHTAB ALAM⁴, (Senior Member, IEEE)

¹School of Electrical Engineering and Computer Science, National University of Sciences and Technology (NUST), Islamabad 44000, Pakistan

²Department of Electrical Engineering, Pakistan Institute of Engineering and Applied Sciences (PIEAS), Islamabad 45650, Pakistan

³Dipartimento di Elettronica, Informazione e Bioingegneria, Politecnico di Milano, 20133 Milan, Italy

⁴Thomas Johann Seebeck Department of Electronics, Tallinn University of Technology, 19086 Tallinn, Estonia

Corresponding author: Rizwan Ahmad (rizwan.ahmad@seecs.edu.pk)

This work was supported by the North Atlantic Treaty Organization Science for Peace and Security (NATO-SPS) under Grant G5482.

ABSTRACT In an event of a disaster, the connectivity of on-scene available User Equipment (UE) to the first responders is important because of the unavailability of conventional networks. Therefore, in this paper, considering the deployment of both the Unmanned Aerial Vehicle (UAV) and Mobile Command Center (MCC), we investigate end to end connectivity of UEs to the MCC in terms of the outage. Specifically, various disaster aware clustering schemes are proposed that utilize the UAV and MCC position for the association. These schemes include multiple degrees of freedom to manage intra-cluster distances along with the flexibility to restructure the clusters. In addition, we assume the provision of simultaneous wireless information and power transfer (SWIPT) at Cluster Heads (CHs) through the UAV and MCC. The results show that the association of a UE to MCC or UAV prior to clustering can be optimized to achieve better performance. Without SWIPT at CH, the minimum distance metric to the UAV provides less outage. However, with SWIPT a weighted compromise between intra-cluster distance and CH distance to the UAV achieves less outage. We applied our proposed methods on a real man-made disaster scenario layout and determined their efficacy.

INDEX TERMS Public safety networks (PSNs), energy harvesting, clustering, SWIPT.

I. INTRODUCTION

In disaster situations such as earthquakes, torrential rains, tsunamis, floods, and landslides, one of the biggest problem is the failure of communication infrastructure that makes the responders task difficult. More than often this leads to a large number of trapped victims. Similar situations have also been observed in the case of man-made disasters such as terrorist attacks and hostage situations. According to a report of the National Disaster Management Authority (NDMA) on Oct. 2005 earthquake in Pakistan, there were more than 73,000 casualties, 79,000 people were injured and more than 3.5 million people were adversely affected. Most of the initial rescue and relief efforts were slow due to the loss of communication network infrastructure and limited access to the disaster area [1]. Similarly, in July 2010 the excessive rains led to floods and landslides. There were more than 2000 casualties, 3000 were injured and approximately twenty

million people were affected [2]. On Oct 10, 2009, around 10 militants attacked Pakistan Army General Headquarters (GHQ), which caused around six casualties and more than twenty people were held hostage [3]. Similar disaster situations have also been observed worldwide, such as Australian bushfire, Puerto Rico Earthquakes, Amazon Wildfires, Tropical Storm Imelda and etc [4]. Therefore, to manage search and rescue operations, the resilient and self-sustainable Public Safety Networks (PSNs) are required.

The success of PSNs lies in the exchange of information between the on-scene available devices and the first responders such as firefighters, police, armed forces, counter-terrorism forces, health and paramedic staff, etc. As it is very important to acquire first-hand information about the number of people affected in the area, their locations, and other critical information. When on-scene devices are unable to communicate with the base station (BS) directly due to the failure of traditional infrastructure, one of the possible solution is to use cooperative device-to-device (D2D) communications to reach the BS or a temporarily deployed

The associate editor coordinating the review of this manuscript and approving it for publication was Ding Xu¹.

Mobile Command Center (MCC) [5]–[7]. For effective communications across the network, a set of devices can be grouped into clusters to minimize transmission overhead and improve the energy efficiency of the network [8]–[10]. It is further envisioned that the average number of hops in a D2D cooperative network can be reduced by using Unmanned Aerial Vehicle (UAV). For example, the authors in [11] proposed multi-layered network architecture for the placement of UAV and association of on-scene devices with the focus on energy efficiency. Recently, a distributed power allocation scheme for disaster communications that uses a UAV and the K-means clustering approach is discussed in [12].

One of the most important aspects in D2D disaster networks is to ensure the information flow (with minimum outage) to the MCC using the minimum number of hops and energy. The clustering helps in conserving the energy of on-scene devices. However, this leads to an increase in the average number of hops in the network. Multiple D2D hops make the information flow more susceptible to outage, which can lead to network failure. Also, the power requirements to maintain an active connection can vary significantly with in the network because of the position of on-scene devices (trapped victims hiding under the tables, behind the cabinets and counters etc). To this end, Energy Harvesting (EH) can play a key role in maintaining the connectivity by supplementing the battery power in disaster scenarios/PSNs [13]–[18]. In disaster situations, energy accessibility, efficiency, reliability are very important, therefore, the use of solar and wind energy is not feasible [19], [20]. However, RF-EH is a promising technique that can enable Simultaneous Wireless Information and Power Transfer (SWIPT).

Mainly, SWIPT has two protocols for EH that are Time Switching (TS) and Power Splitting (PS). In TS, the transmission period is divided into two parts: the first part is used for EH and the second part is used for transmission of data. PS divides the received signal power into two parts; the first part is used for EH and the second part is used for transmission of the data [21]–[23]. In literature, non-linear energy harvesting model [24] was also proposed for SWIPT systems, which is more realistic than existing linear energy harvesting models.

The authors in [25] used SWIPT for the throughput maximization of a simple cooperative network in which the UAV acts as a relay. Although this algorithm optimizes transmission power, PS ratio, and the UAV trajectory, it is not directly applicable in disaster scenarios where there may be multiple devices and some of them may not be able to communicate with the UAV or MCC directly. The UAV was also be used for wildfire disaster scenarios to improve reliability of the networks [26]. In [27], the authors proposed the idea of D2D communication for coverage extension from a disaster (non-functional) area to a functional area through relay nodes. This work shows the benefit of clustering in reducing energy consumption and increasing the network lifetime using TS SWIPT. However, this work did not consider the impact of UAVs.

The above literature establishes the utility of incorporating clustering, UAVs, and SWIPT for disaster and other communication scenarios [28]–[33]. SWIPT is used to supplement the energy of cluster heads (CHs) since they forward data reliably to its cluster members (CMs). In disaster networks one of the major requirement is to provide maximum end to end connectivity. Another benefit of SWIPT is to allow the selected CHs to operate in a stable state without causing CH/Network reconfiguration. SWIPT may increase the effective communication and network life time of the scenario and on other hand, it is also a promising technology in terms of wireless security [34]–[39]. However, the existing literature only considers the connectivity between the UAV and devices and often ignores the role of MCC, which may be able to provide partial coverage to the devices near its vicinity. In addition, the UAV backhaul to the BS/MCC [27], [40]–[42] is also not considered, which can significantly impact the performance in the case of a large disaster area. All these factors can significantly alter the clustering process in the disaster area. Therefore, in this paper, we present a unified clustering approach for the UAV and SWIPT assisted disaster networks and make the following contributions.

- Considering MCC as a backhaul to the UAV, the following clustering schemes are devised, i) Clustering without association that does not consider the presence of MCC and UAV, ii) Clustering with the association that considers the presence of both the MCC and UAV.
- In clustering with association scenario, five different variants of CH selection and Cluster Member CM) association are proposed based on the UAV and MCC positions and coverage areas.
- Considering the provision of Hybrid Energy Harvesting (HEH) on CHs, the average end to end outage is calculated for all the clustering schemes. The results are compared with non-HEH clustering schemes.
- A case study of a real terrorist attack scenario is carried out (using an asymmetric layout with open spaces) to validate the efficacy of the clustering schemes with and without the provision of HEH.

The rest of the paper is organized as follows: Sec II describes the generic system model for disasters including the provision of HEH. Sec III provides a detailed description of the clustering schemes. A detailed simulation study of these schemes is provided in Sec IV. Finally, Sec V presents the conclusion and future directions.

II. SYSTEM MODEL

Fig. 1 depicts a disaster scenario in which the cellular network becomes unavailable and the victims carrying the user equipment (UE) devices are unable to communicate with the responders. We consider that the M randomly distributed UEs can support D2D communication through multiple interfaces such as legacy Wi-Fi, Wi-Fi Direct, LTE- Direct, and BLE [43]–[45]. The on-scene available UEs must be able to

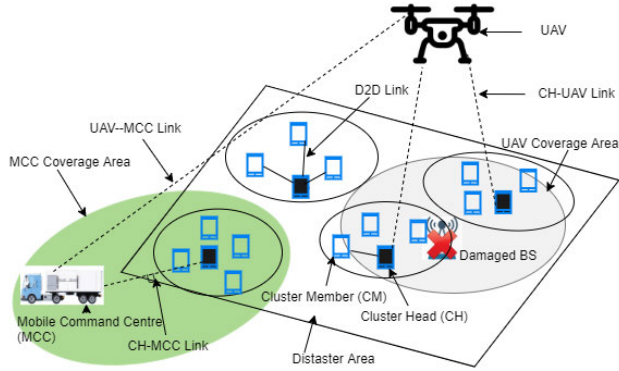


FIGURE 1. Proposed model framework for disaster recovery communication using D2D, clustering.

discover each other within their proximity.¹ The UEs use the proximity information and group themselves in the form of clusters. The provision of multiple wireless interfaces enable UEs to establish an interference free network (including both intra and inter cluster interference).

The distance and energy information is used to designate the UE as a CH or a CM. All the information of a CM is routed through a CH. The temporary connectivity of the UEs to the responders is ensured through the deployment of MCC. In order to reduce the hops for the CHs to reach MCC, a UAV is deployed in the disaster area. The UAV acts as a relay for CHs to reach MCC. It is further assumed that all the UEs are able to harvest energy from the UAV and MCC.

It is assumed that the channel gain on CH-CH, CH-MCC, and CH-UAV links follow Rayleigh distribution, whereas, the channel gain between UAV-MCC follow Rician distribution [46]. A list of important acronyms and symbols is presented in Table 1. To generalize, we consider u as a source and v as a destination in the bidirectional links (CH-CH, CH-MCC, CH-UAV, and UAV-MCC), d_{u-v} as the distance between them, $P_{tx,u-v}$ as the transmit power of the source, μ is the path loss exponent, R_{u-v} as the transmission rate, and h_{u-v} as the channel gain. The received power and the capacity of the link is given as

$$P_{rx,u-v} = \frac{P_{tx,u-v}|h_{u-v}|^2}{d_{u-v}^\mu}, \quad (1)$$

$$R_{u-v} = B \log_2 \left(1 + \frac{P_{tx,u-v}|h_{u-v}|^2}{\sigma^2 d_{u-v}^\mu} \right). \quad (2)$$

where, B is the channel bandwidth and σ^2 is the noise power.

A. HYBRID ENERGY HARVESTING PROTOCOL

In this work, we consider a SWIPT mechanism at CH as it is responsible for forwarding data. The SWIPT mechanism can

¹In the existing LTE-A network, a UE can only discover nearby UEs through the synchronization signal (PSS/SSS) and their coordinates can be found based on the RSSI values. With the help of coordinates, we can easily calculate the approximate location of available UEs. Due to the constraints of the receiver sensitivity, the UEs cannot communicate their information to the MCC directly.

TABLE 1. Acronyms and symbols.

Symbols	Descriptions
MCC	Mobile Control Centre
UAV	Unmanned Aerial Vehicle
UE	User Equipment/ Devices
M	Total Number of UEs
K	Number of Clusters associated with UAV
J	Number of Clusters associated with MCC
CH	Cluster Head
CM	Cluster Member
D2D	Device to Device
RF	Radio Frequency Signal
EH	Energy Harvesting
SWIPT	Simultaneous Wireless Information and Power Transfer
TS	Time Switching
PS	Power Splitting
HEH	Hybrid Energy Harvesting
$P_{tx,u-v}$	Transmit Power of UEs
P_s	Source Transmit Power
d_{u-v}	Distance between MCC-CH, UAV-CH, CH-CH, CH-CM
μ	Path Loss Exponent
R_{u-v}	Transmission rate
h_{u-v}	Link channel gain MCC-CH, UAV-CH, CH-CH, CH-CM
$P_{rx,u-v}$	Received Power at Destination
B	Channel Bandwidth
σ^2	Noise Power
α	Time Switching Factor
λ	Power Splitting Factor
T	One Block Time Period
ζ	Energy Efficiency Factor
E_{th}	Threshold required for activate the energy harvesting circuit
E_H	Energy Harvesting at CH Nodes
$P_{tx,ch-v}$	Transmit Power of Signal between CH-CM
P_o	End to End Outage Probability
P_{th}	Received Power Threshold

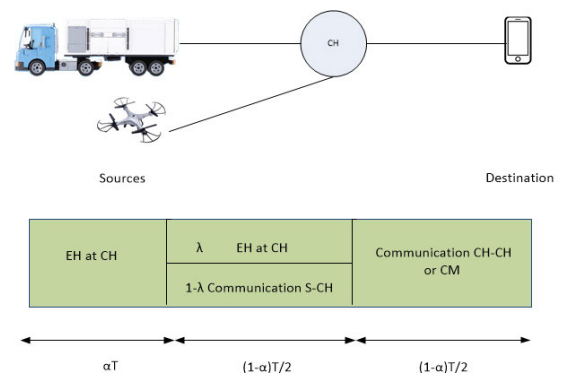


FIGURE 2. Hybrid energy harvesting protocol.

be categorized as TS, PS, and HEH protocol. HEH allows two degrees of freedom to control EH and data forwarding, therefore, it has wider applicability in scenarios with a single EH source. Fig. 2 shows a HEH protocol at CH, assuming T as the total time for a single transmission phase from sources (UAV, MCC)-CH-destinations (other CHs or its CM). HEH consists of the following three steps.

- Step 1: For $(\alpha)T$ time, the CH harvests RF energy from either the UAV or MCC. The value of α varies between 0 and 1.
- Step 2: For $\left(\frac{1-\alpha}{2}\right)T$ time interval the source (UAV, MCC) communicates its information to the CH node. The factor λ defines the fraction of the energy that CH harvests from the source received signal. The HEH in this time interval depends on the received signal strength. The value of λ also varies between 0 and 1.
- Step 3: For the remaining $\left(\frac{1-\alpha}{2}\right)T$, the CH communicates with destination. The destination can be other CHs or its CMs.

The choice of α and λ enables different HEH scenarios which are given below.

- $\alpha = 0$ and $\lambda = 0$ indicate that there is no HEH at CH;
- $\alpha = 1$ and $\lambda = 0$ indicate only the TS is applied at CH;
- $\alpha = 0$ and $\lambda = 1$ indicate only the PS is applied at CH;
- $0 < \alpha < 1$ and $0 < \lambda < 1$ indicate both the PS and TS are applied at CH.

Suppose h_{s-ch} and d_{s-ch} is the channel gain and distance between the source (UAV or MCC) to the CH (to which it is associated to), respectively, $P_{tx,s-ch}$ is the source power $s \in \{mcc, uav\}$, and ζ is the energy efficiency factor, then the HEH at any CH which is associated with the UAV in Step 1 is given as

$$E_1 = \frac{\alpha T \zeta P_{tx,uav-ch_k} |h_{uav-ch_k}|^2}{d_{uav-ch_k}^\mu}, \quad (3)$$

The HEH during Step 2 is becomes

$$E_2 = \frac{(1-\alpha)T \zeta P_{tx,uav-ch_k} \lambda |h_{uav-ch_k}|^2}{2d_{uav-ch_k}^\mu}, \quad (4)$$

The total HEH during a single transmission phase is

$$E_H = E_1 + E_2, \quad (5)$$

The energy accumulated is used to supplement the transmission power of the UE in the transmission slot. The E_H is fully consumed during each transmission phase.

$$E'_{tx,ch_k-v} = E_{tx,ch_k-v} + E_H, \quad (6)$$

where, E_{tx,ch_k-v} is corresponding to P_{tx,ch_k-v} in (2) and the following equation provides the power transmitted in HEH scenario.

$$P'_{tx,ch_k-v} = \frac{2E'_{tx,ch_k-v}}{(1-\alpha)T}. \quad (7)$$

We define the area around the MCC and UAV where the energy is harvested is called HEH area, which is circular and radius of the circle is given by

$$R_{EH} = \left(\frac{\zeta P_s}{E_{th}}\right)^{\frac{1}{\mu}}. \quad (8)$$

where $s \in \{UAV, MCC\}$ and E_{th} is the EH threshold that activates the HEH.

B. AVERAGE OUTAGE PROBABILITY

In this paper, we are interested in an average end to end outage $E(P_o)$ of M UE's, where $E(\cdot)$ is an expectation operator and P_o is the end to end outage probability. This term represents an average outage between a UE and MCC, when the UEs are randomly distributed in the disaster area. If u and v represents the source and destination in the i^{th} hop, the outage probability is defined as

$$P_{o,i} = \Pr(P_{rx,u-v} \leq P_{th}), \quad (9)$$

where, P_{th} is the outage threshold.

$$P_{o,i} = \Pr\left(\frac{P_{tx,u-v} |h_{u-v}|^2}{\sigma^2 d_{u-v}^\mu} \leq P_{th}\right), \quad (10)$$

and

$$P_{o,i} = \Pr\left(|h_{u-v}|^2 \leq \frac{P_{th} \sigma^2 d_{u-v}^\mu}{P_{tx,u-v}}\right) = 1 - e^{-\left(\frac{P_{th} \sigma^2 d_{u-v}^\mu}{P_{tx,u-v}}\right)}.$$

In a multihop scenario, the outage at any hop is considered as an end to end outage. This is explained in Table 2, where a two hop scenario is explained. For a general multihop scenario, end to end outage probability P_o can be written as

$$P_o = 1 - \prod_{i=1}^{noofhops} P_{o,i}. \quad (11)$$

TABLE 2. Outage cases.

Hop 1 Outage	Hop 2 Outage	End to End Outage
Yes	Yes	Yes
Yes	No	Yes
No	Yes	Yes
No	No	No

If the last hop is between UAV and MCC, the exponential term is replaced by the Cumulative Distribution Function of Rician distribution. Since the UE's are distributed randomly in a disaster area, the calculation of average end to end outage requires averaging over the distribution of randomly formed hops from a UE to MCC and corresponding hop distances. In the following, considering the limited transmit power capability of the UE's, we propose disaster aware clustering schemes that utilize the UE association and non-association with the MCC and UAV to minimize outage probability.

III. DISASTER REGION CLUSTERING AND ASSOCIATION

This section presents the disaster aware clustering techniques that consider the presence of both the UAV and MCC. The clustering algorithms are based on modified a K-means algorithm (K-means and elbow algorithm) and incorporates the UEs receiver sensitivity and energy constraints. It is well known that the K-means computational complexity is $O(M(\Delta + L))$, where M is the number of nodes, Δ is dimension (because clustering is based on distance, the dimension is 2), L is the total number of clusters, K is the number

of clusters associated with UAV and J is the number of clusters associated with MCC. Since, we are using elbow algorithm to find the optimal number of clusters, it means that clustering algorithm has to run L times starting from $l = 1$. The computational cost then becomes $\sum_{l=1}^L O(M(\Delta + l)) = O(\sum_{l=1}^L M(\Delta + l))$. While considering different disaster situations, we propose two main approaches to ensure the end to end connectivity, namely, clustering without association (CWoA) and clustering with the association (CWA). In addition, five more clustering schemes are also derived from CWoA and CWA. The clustering process requires the location coordinates of all the UEs and the number of clusters as inputs. The number of clusters associated with the MCC and UAV is denoted by J and K respectively. The optimal number of clusters for UEs are obtained using the Elbow algorithm. In the Elbow algorithm, starting from an initial $K = 2$ ($J = 2$), CMs and the sum squared error of their distance from centroid is calculated. The value of K and J is increased in an iterative manner until the change in sum squared error becomes insignificant. As depicted earlier, this value of K and J will be used as an input to the clustering process.

To cluster the UEs, first, the centroids' location of K clusters are randomly selected. Secondly, the mean distances between the centroids and every UE of the cluster are calculated. The UE will associate itself to the nearest centroid. Once this process is completed, centroids are recalculated based on its associated UEs. This step will be repeated when the change in centroid location is negligible compared to that in the previous step. Once the centroids of the clusters are calculated, the UE closest to the centroid is declared as the CH provided that its energy is greater than the threshold. If the closest UE's energy is less than the threshold, the next closest UE to the centroid is selected with energy greater than the threshold. If in a cluster no UE has the energy greater than the threshold, the closest UE is declared as the CH. Once a cluster is associated with the MCC/UAV, all the traffic originating from that cluster is routed to MCC/UAV respectively. The routing of this traffic may involve multiple hops.

- **Clustering without Association (CWoA):** In this CWoA approach, the clustering of UEs in the disaster region is carried out without considering the deployment of the UAV and MCC. This approach is useful in the immediate aftermath of the disaster as the UAV and MCC might not be readily available. Once the UAV and MCC are deployed, the CHs associate themselves either to the UAV or MCC based on the minimum distance. This approach is referred to as CWoA.
- **Clustering without Association (CWoA)-E:** Similar to the above approach clustering is performed without considering the deployment, however, there may be situations in which it is not possible for the MCC to be in close proximity to the disaster region such as terrorist attacks. In these situations, the MCC may not be able to provide extended coverage to the disaster area. Subsequently, the minimum distance rule may not be

applicable. Therefore, while associating CHs we also consider the possibility of MCC's limited coverage. The association in this scenario is carried out by defining an MCC exclusive zone (CWoA-E). The CHs in the MCC exclusive zone are associated with the MCC, whereas the remaining CHs associate themselves to the UAV. The CHs in MCC exclusive zone can send the data directly to the MCC without taking any hops.

- **Clustering with Association (CWA):** In a simple CWA approach, considering the deployment of both the UAV and MCC, the association is carried out before clustering. Similar to CWoA-E, the UEs within the MCC exclusive zone are associated with the MCC, and the rest of the UEs are associated with the UAV. The set of UEs associated with the MCC and UAV are then clustered independently. This approach is applicable in areas susceptible to disasters, where emergency setups are readily available. The disaster area is known whereas the number of users are unknown. Therefore, clustering is carried out after associating the UEs with the MCC or UAV. The number of clusters associated with the UAV is denoted by K and the number of clusters associated with MCC is denoted by J .
- **Clustering with Association-Weighted (CWA-W):** In this approach, initially, a centroid and the nodes of a cluster are found using CWA approach. The CH selection within the cluster is based on a metric that is a weighted combination of nodes' distances from the centroid and their respective distances to the UAV or MCC. Let $d_{(k,1)-c_k}, d_{(k,2)-c_k}, \dots, d_{(k,M_k)-c_k}$ are the distances of CMs from the centroid and $d_{(k,1)-uav}, d_{(k,2)-uav}, \dots, d_{(k,M_k)-uav}$ are the distance of CMs from the UAV, the weighted CWA-W metric for UAV $k \in 1, \dots, K$, and $m_k = 1, \dots, M_k$ where m_k is number of cluster associated with UAV is given as

$$D_{k,m_k}^{uav} = \beta \frac{d_{(k,m_k)-c_k}}{\max(d_{(k,1)-c_k}, d_{(k,2)-c_k}, \dots, d_{(k,M_k)-c_k})} + (1-\beta) \frac{d_{(k,m_k)-uav}}{\max(d_{(k,1)-uav}, d_{(k,2)-uav}, \dots, d_{(k,M_k)-uav})} \quad (12)$$

where, β is the weighting factor. Similarly, the above metric can be applied to MCC with J clusters $j \in 1, \dots, J$, and $n_j = 1, \dots, N_j$ where n_j is number of cluster associated with MCC as,

$$D_{j,n_j}^{mc} = \beta \frac{d_{(j,n_j)-c_j}}{\max(d_{(j,1)-c_j}, d_{(j,2)-c_j}, \dots, d_{(j,N_j)-c_j})} + (1-\beta) \frac{d_{(j,n_j)-mc}}{\max(d_{(j,1)-mc}, d_{(j,2)-mc}, \dots, d_{(j,N_j)-mc})} \quad (13)$$

Fig. 3 explains this weighted CWA (CWA-W) approach. Unlike the CWA approach, the CH is not

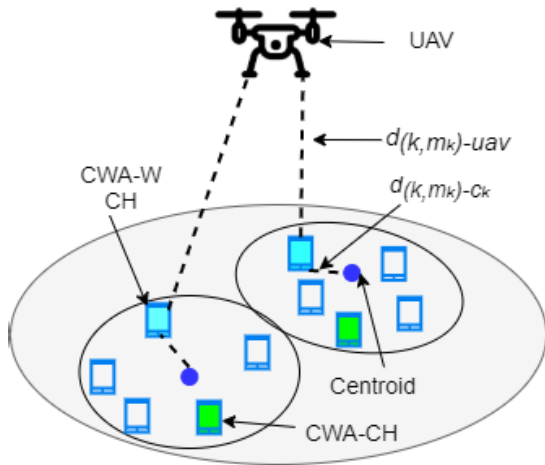


FIGURE 3. Clustering scheme CWA-W.

selected from its minimum distance to the centroid. For the selection of CH, the value of β calculates a metric for each temporary CM. The CM with the minimum value of D_{k,m_k} becomes the CH of the cluster k .

- **Clustering with Association-Minimum Distance (CWA-MD):** From equation (12), when the value of $\beta = 0$, the CM with a minimum distance to the UAV or MCC will become a CH. Due to this fact, CWA-W for $\beta = 0$ is referred to as CWA-MD.
- **Clustering with Association-Modified Metric (CWA-MM):** The CWA-W approach changes the position of CH node within a cluster based on the value of β and does not consider association to other clusters based on their distance to the UAV or MCC. Also, CWA-W tends to move the CH closer to MCC or UAV and makes the CM to CH distance more asymmetrical. This may result in higher EH at the CH, however, some CMs suffer higher distance dependent path loss. In essence, CWA-W is a local approach. Therefore, we propose a two step clustering approach that consider the re-association of CMs to other centroids. Initially, the clustering is performed using CWA and temporary centroids and CMs are identified. Afterward, a modified metric for CM re-association is defined that takes into account their distance from the temporary CHs and the distance of temporary CHs to the UAV or MCC. Let $d_{(k,m_k)-c_1}, d_{(k,m_k)-c_2}, \dots, d_{(k,m_k)-c_K}$ are the distances of m_k node of k^{th} temporary CM from every centroid and $d_{c_1,uav-uav}, d_{c_2,uav-uav}, \dots, d_{c_K,uav-uav}$ are the distance of every centroid from the UAV, then the re-association metric for $k \in 1, \dots, K, m_k = 1, \dots, M_k$ is defined as

$$D'_{k,m_k,uav} = \delta \frac{d_{(k,m_k)-c_k}}{\max(d_{(k,m_k)-c_1}, \dots, d_{(k,m_k)-c_K})} + (1 - \delta) \frac{d_{c_k-uav}}{\max(d_{c_1-uav}, \dots, d_{c_K-uav})} \quad (14)$$

The m_k node of the k^{th} temporary cluster will calculate $D'_{k,m_k,uav}$ for all centroids and associates with a centroid c'_k having minimum value of $D'_{k,m_k,uav}$. Fig. 4 explains the CWA-MM re-association process for UAV, in which temporary centroids are calculated as in the CWA approach. A similar process is carried out for MCC. Once these centroids are calculated a CM calculates minimum $D'_{k,m_k,uav}$ and performs re-association. Similarly, the above metric $D'_{k,m_k,uav}$ can also be calculated for MCC clusters by suitably changing the variables.

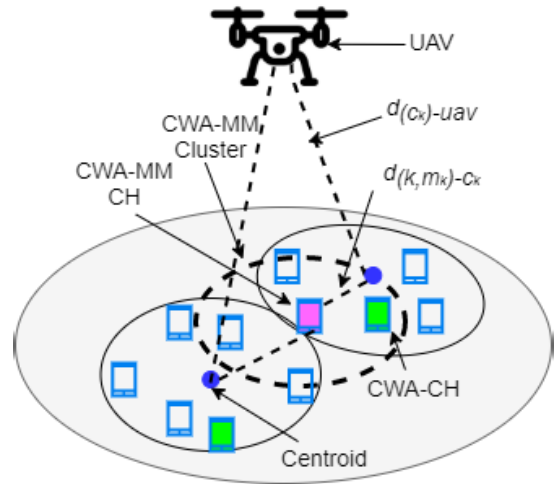


FIGURE 4. Clustering scheme in CWA-MM.

- **Clustering with Association-Weighted Modified Metric (CWA-WMM):** In this three step approach, initially, CMs are decided based on temporary centroids. In the second step, the re-association of CMs is carried out using CWA-MM approach using equation (14). After re-association, the CH selection is carried out based on the CWA-W approach in equation (12).

IV. ANALYTICAL AND SIMULATION RESULTS

We consider a disaster area of $100m \times 100m$ in which UE's are uniformly distributed. The simulation parameters are summarized in Table 3. The simulations are carried out in MATLAB R2019a. We consider two main scenarios for simulation. In the first scenario, it is assumed that the UEs are not EH capable, whereas, in the second scenario EH enabled UE's are considered. In both the scenarios, average end to end outage probabilities from the UE (a CM) to the MCC or UAV is used as a performance metric. We consider that all the links experience independent Rayleigh fading. A case study of a real scenario is also included to determine the efficacy of the proposed clustering approaches.

A. WITHOUT EH, $\alpha = 0, \lambda = 0$

Fig. 6 shows the outage probability of a UE to reach the UAV/MCC for different clustering schemes. The MCC is placed at $(-10, 0)$ and its coverage range for CWoA-E, CWA, CWA-W, CWA-MM, CWA-WMM, and CWA-MD is kept

TABLE 3. Simulation parameter.

Parameters	Values
Area	100 m x 100 m
No of Devices	100-300
B (Bandwidth)	10 Mhz
ζ	1 Mbits
$P_{tx,uv}$	1.425 Joules/s
$P_{rx,uv}$	0.925Joules/sec
Max.UE E_{Tx} power	0.2 Watts
μ	3.2
Rayleigh Parameter	$E[x ^2] = 1$
T	1
α	0-1
λ	0-1
β	0-1
δ	0-1
Noise Power	-90 dBm

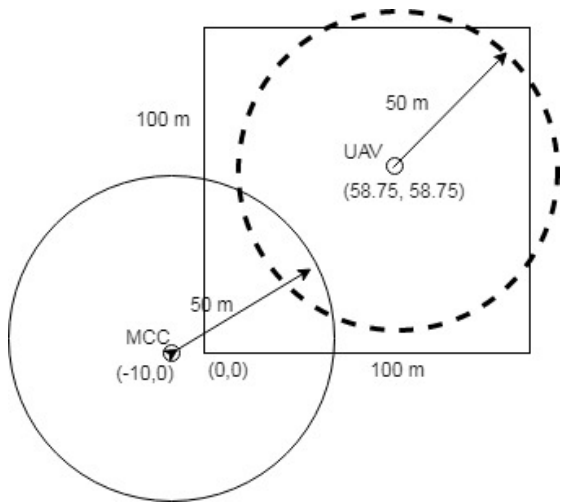


FIGURE 5. Simulation layout.

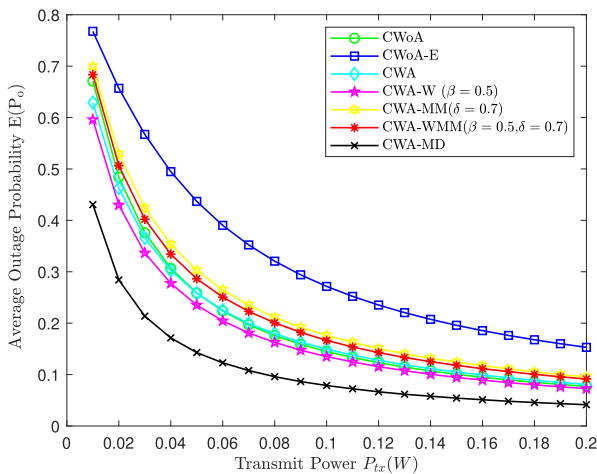


FIGURE 6. Average outage probability versus transmit power of UE's without EH, area (100m x 100m), $\beta = 0.5$, $\delta = 0.7$.

50m as shown in Fig. 5. The position of UAV (58.75, 58.75) is selected such that the maximum disaster area is covered by the MCC and UAV. The EH coverage of UAV (R_{EH}) is calculated from equation (8). The maximum coverage of UAV is restricted to 50m. When the transmit power of the UEs is

varied from 0.01 to 0.2 watts, the CWoA-E performs worst and CWA-MD performs best when compared to all other clustering schemes. The reason for the worst performance of CWoA-E is due to the association of clusters. The clusters in MCC region have to take multiple hops to reach MCC, even though that UAV may be closer. The CWA approach compensates for the outage by first performing association with the UAV and MCC. Since the MCC coverage area is small compared to the coverage region of UAV, the CWA helps in better distribution of the clusters as depicted by the curves of CWA-W, CWA-MM, CWA-WMM, and CWA-MD. Although CWoA-E performs worst in terms of the outage, it is more practical for terrorist scenarios; where the MCC cannot be placed near the disaster area. The CWA-MD approach makes best use of UAV position for creating cluster by minimizing the CH distance to the UAV.

Figs. 7 and 8 shows the impact of the β and δ in CWA-W and CWA-MM schemes, respectively. It can be seen that outage probability increases with β . This is because as β increases the CH selection moves away from the UAV/MCC

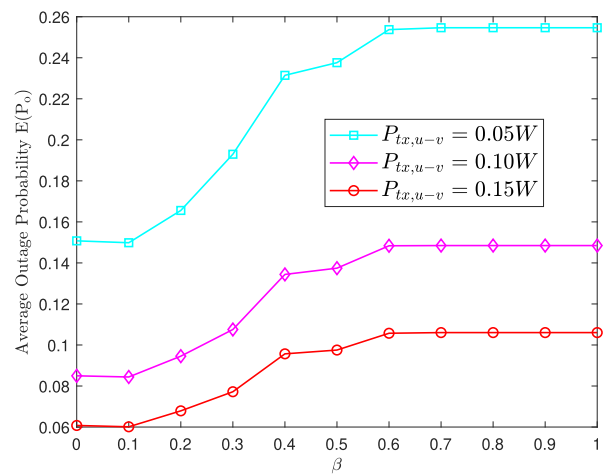


FIGURE 7. Effect of β on average outage probability of CWA-W scheme without EH, area (100m x 100m).

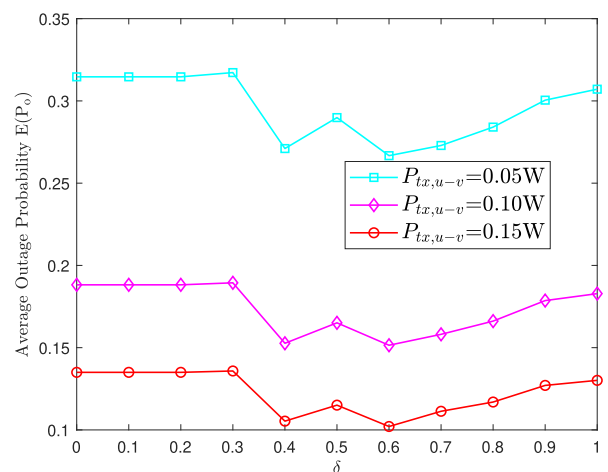


FIGURE 8. Effect of δ on average outage probability of CWA-MM scheme without EH, area (100m x 100m).

and outage on the CH to UAV/MCC link increases. Note that $\beta = 0$ will result in a CH selection that is closest to the UAV, whereas, $\beta = 1$ will result in a CH selection that is closest to the conventional K-mean centroid. The δ in CWA-MM has a different effect compared to β , and the outage probability shows the increasing and decreasing trends. This is because the CWA-MM approach allows the re-association of the UEs to other centroids and highly dependent on the distribution of UE's. When δ approaches 1, CWA-MM approaches CWA and when δ approaches 0, the UE's re-associate to the centroids with minimum distance to the UAV. These extreme values of δ results in higher path loss; CM to CH when $\delta = 0$ and CH to UAV when $\delta = 1$ (as shown in equation (14)). The net outcome is a higher outage probability as shown in Fig. 8. The middle values of δ provide a better trade-off between the CM to CH and CH to UAV/MCC path losses.

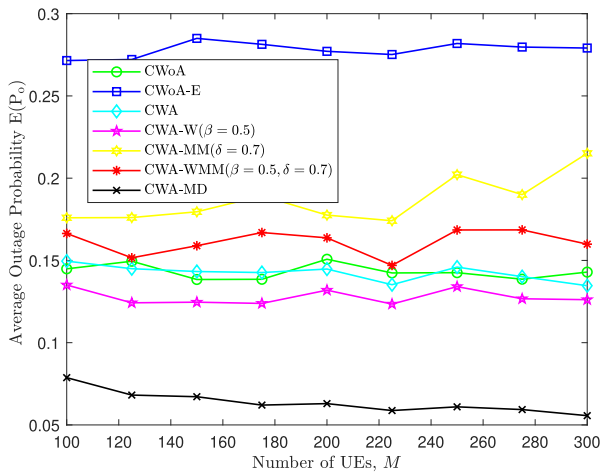


FIGURE 9. Average outage probability versus the number of UE's, area (100m x 100m), $\beta = 0.5$, $\delta = 0.7$.

Fig. 9 shows the outage probability curves of different clustering schemes with an increasing number of UEs. The results indicate a convergence of the proposed schemes in terms of outage probability. These curves do not change significantly as the UE density is relatively high, which inhibits any changes in cluster formation. Only small changes in CWA-MD and CWA-MM are noteworthy. Of course, the increase in the disaster-region will also change the trends observed here. Fig. 10 shows the impact of outage probability when the disaster area increases to $200m \times 200m$. Intuitively, the outage probability increases for given transmit power and the number of UEs. The CWoA-E approach becomes infeasible, whereas all the remaining clustering schemes perform consistently with the transmit power. The CWA-MM has lower outage probability compared to CWA-WMM, which is different from the observations in Fig. 6. The CWA-MD is the best possible clustering approach.

B. WITH EH, $\alpha \neq 0$, $\lambda \neq 0$

Fig. 11 shows the total network outage of EH capable devices. The UEs harvests energy from the UAV through HEH (TS & PS) with $\alpha = 0.33$ and $\lambda = 0.5$. The UEs use

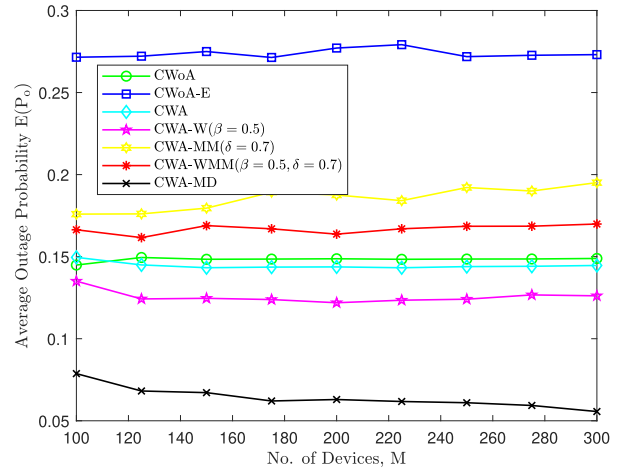


FIGURE 10. Average outage probability versus transmit power of the UE's without EH, area (200m x 200m), $\beta = 0.5$, $\delta = 0.7$.

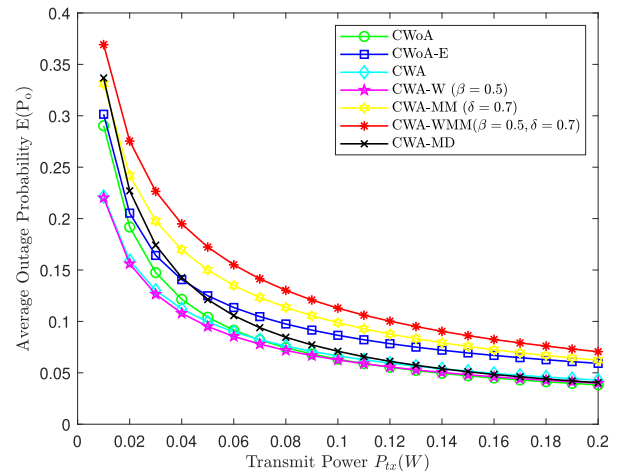


FIGURE 11. Average outage probability versus transmit power of the UE's with HEH, area (100m x 100m), $\beta = 0.5$, $\delta = 0.7$.

the energy from HEH to augment their transmission power. Therefore, the transmit power of UE can be divided into two energy components: basic energy (battery) and HEH. Since HEH is variable, the figure plots outage probabilities against the transmit power corresponding to basic energy. However, as described earlier the transmit power is the sum of the battery power and the power derived from HEH.

Compared to Fig. 6, the same schemes in Fig. 11 behave differently due to the provision of HEH. The CWA-WMM gives the highest outage whereas the CWA and CWA-W provide the minimum outage. The outage performance of CWA-WMM is mainly due to the re-association of the UEs with other centroids. On average, this results in bigger cluster size, and the outage probability is dominated by the CH to CM links. The CWA-W ensures the proximity of the CH with the UAV/MCC and CM. Compared to Fig. 7, the outage probability in Fig. 12 decreases with increasing β . The increasing value of β moves the CH closer to the K-means centroid and the distances become more symmetrical with respect to CH (on average lower CH to CM distances). This indicates that for a given scenario, the HEH component doesn't

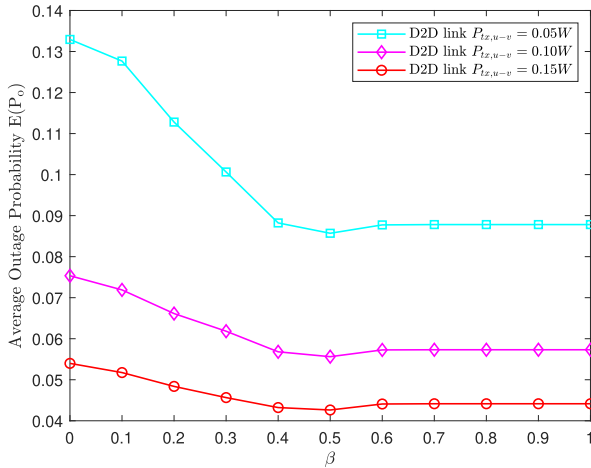


FIGURE 12. Effect of β on average outage probability of CWA-W scheme with HEH, area (100m x 100m).

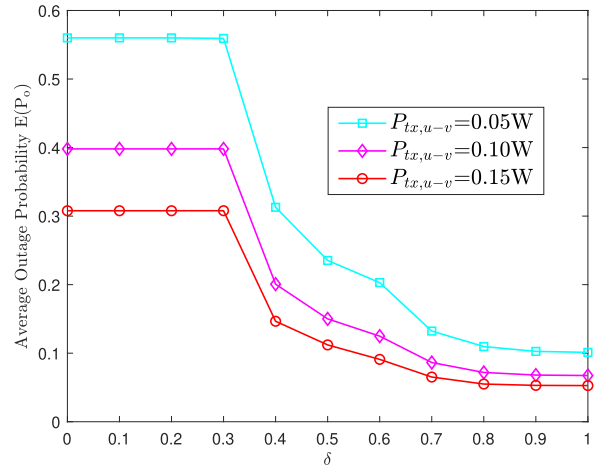


FIGURE 14. Effect of δ on average outage probability CWA-MM scheme with HEH, area (100m x 100m).

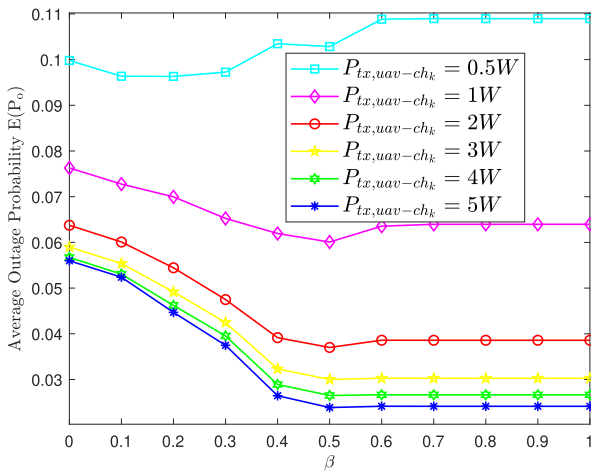


FIGURE 13. Effect of β on source power in CWA-W, transmit power of UE's = 0.1W, area (100m x 100m).

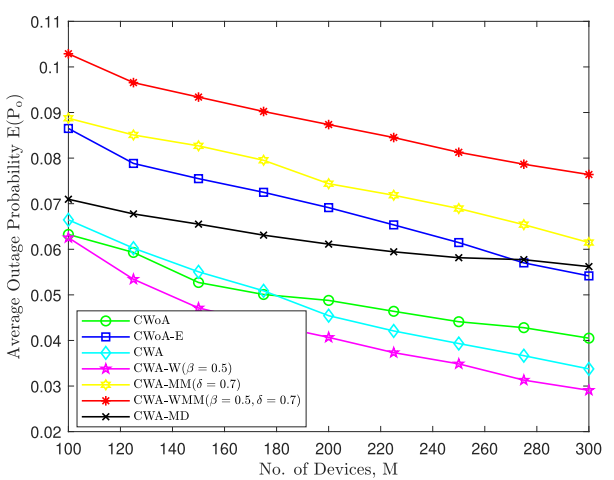


FIGURE 15. Average outage probability versus no of UE's, area (100m x 100m), $\beta = 0.5, \delta = 0.7$.

change significantly across the cluster. This observation is also demonstrated by Fig. 13 in which outage probability curves of CWA-W decreases with increasing β when source power (UAV/MCC) is high. However, when the source power is low the HEH will fluctuate significantly within the cluster. The outage probability initially decreases and then saturates when the CH selection closer to the centroid (increasing β).

Fig. 14 shows the outage probability curves of CWA-MM by changing δ . The curves remain constant for values of δ up to 0.3 and decrease sharply until they saturate at $\delta = 0.8$. Note that the behavior of the curves for $\delta > 0.3$ is different from that in Fig. 8. When δ is near 1, the UE is likely to stay with the current centroid as opposed to its lower values. In CWA-MM higher values of δ are much feasible. Fig. 15 plots the outage curves with the increasing number of UEs. We can see that the CWA-MD remains almost constant, whereas the outage of other schemes generally shows a decreasing trend with slight fluctuations. The main reason is as UE density increases, there are more cluster formations (elbow algorithm) which means lower intra-cluster distances and subsequently lower outages.

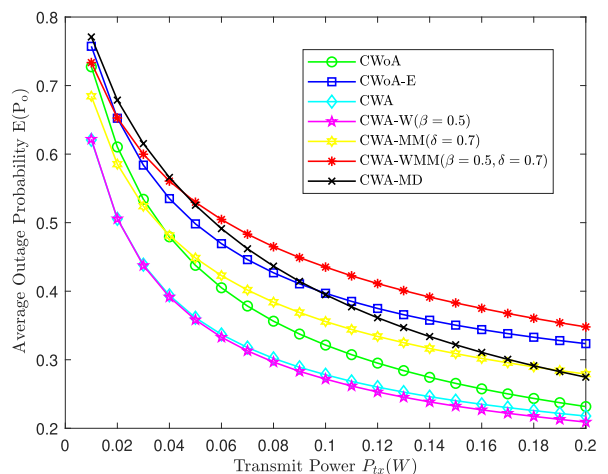


FIGURE 16. Average outage probability versus transmit power of UE's with HEH, area (200m x 200m), $\beta = 0.5, \delta = 0.7$.

Fig. 16 shows the impact of the area on the outage probability of different clustering schemes. One can see that CWA and CWA-W still perform better compared to other schemes with the slightly higher outage. However, the CWA-MD suffers

the most as its outage curve is no more near to the CWA or CWA-W at higher transmit powers. This is mainly due to the fact that CH is closer to the UAV than the centroid. In a relatively larger area (compared to Fig. 11 all the CMs now have to overcome larger path losses. The restructuring of clusters in CWA-MM leads to better performance compared to CWA-MD, CWoA-E, and CWA-WMM. The CWA-WMM though carries the same parameter δ from CWA-MM, however, incorporating β makes the CH position more skewed in a restructured cluster and hence the higher outage probability.

Figs. 17 and 18 shows the impact of source power (UAV/MCC) and disaster area on the outage probability of different clustering schemes. CWA-W provides the best performance, whereas the behavior of other schemes are dependent on the chosen parameters. Relatively, the outage of CWA-MM improves over CWoA-E in a larger disaster area for all transmit powers. In contrast to Fig. 17, the outage curve of CWoA in Fig. 18 is higher than the CWA curve due, due to the larger disaster area.

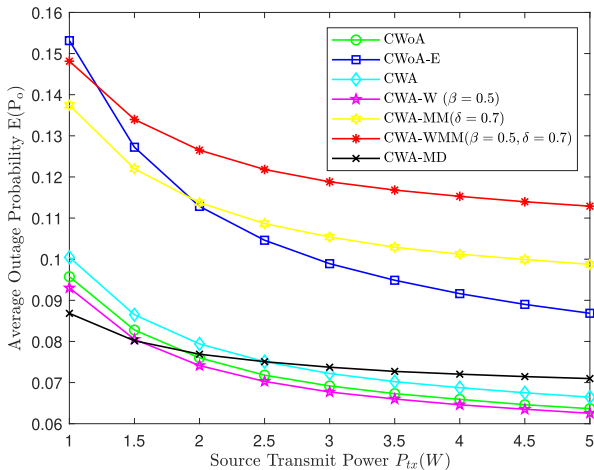


FIGURE 17. Average outage probability versus source power, transmit power of the UE's = 0.1W, area (100m x 100m), $\beta = 0.5$, $\delta = 0.7$.

C. CASE STUDY

In this section, we apply the proposed clustering schemes to the real layout of the Army Public School (APS), Peshawar terrorist attack in 2014. The layout of the APS Peshawar at the time of the terrorist attack is shown in Fig. 19. The reference locations of these buildings have been obtained from the BBC article [47]. New structures have been added since the attacks in 2014. In APS there are many populated buildings namely school Wing, college wing, Classrooms, auditorium, administrative block. The approximate dimensions of these buildings are obtained from Google Earth. We apply the same assumptions as described in the Section. II that there is a complete outage of cellular communication infrastructure to disrupt any communication between the terrorists. Therefore, based on the above assumptions and ground realities the on-scene available devices can not communicate directly to the responders without any infrastructure support. The assumptions based on our proposed solution enable the

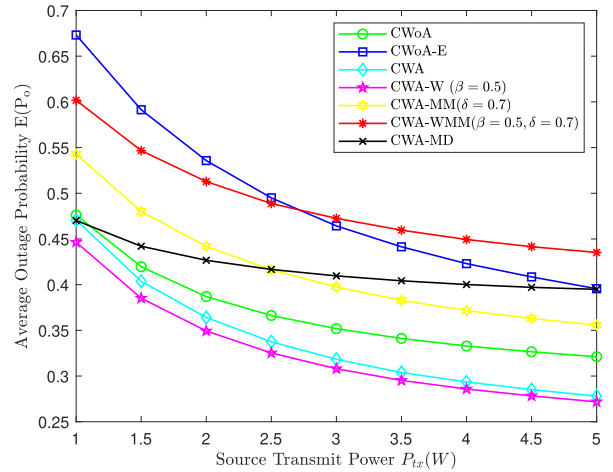


FIGURE 18. Average outage probability versus source power, area (200m x 200m), $\beta = 0.5$, $\delta = 0.7$.

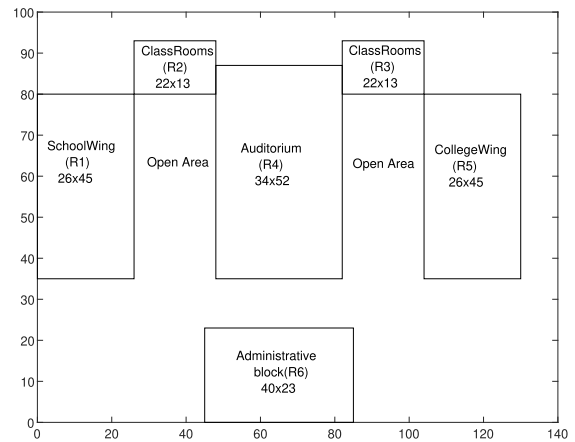


FIGURE 19. Layout of APS Peshawar building.

devices to communicate with the first responders via D2D communication. The on-scene available devices support multiple interfaces like LTE-A, LTE-D and Wifi direct.

Fig. 20 shows the position of UAV and MCC along with a clustered scenario. The dimensions of the scenario are (130m, 93m) The MCC is located at (25m, -15m), which is accessible through the main road. The UAV height is 10m

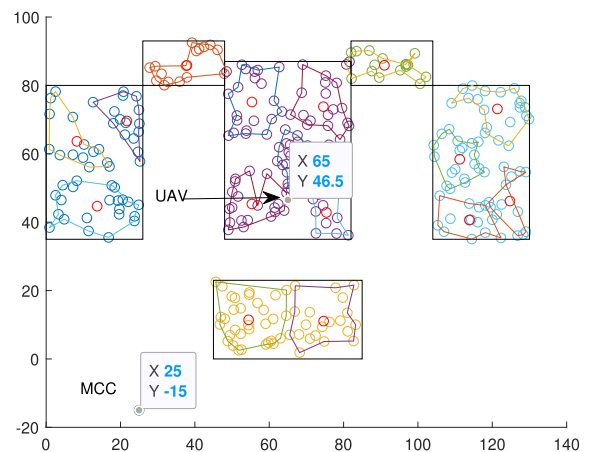


FIGURE 20. Clustering in APS Peshawar building.

and it is placed at the center of the attack scenario, i.e. (65m, 46.5m) (top of the auditorium). The outage probability curves are shown in Fig. 21 for $\alpha = 0, \lambda = 0$. The CWA-MD and CWoA-E provide the lowest and highest outage probability, respectively. The remaining schemes present a slightly different comparison to their curves in Figs. 6. For example, CWA-MM in the APS case provides the second lowest outage probability whereas in Fig. 6 it provided the second highest outage probability. Changing the number of devices has no effect on the outage consistency of the clustering schemes as shown in Fig. 22. This behavior is indicative of clustering convergence.

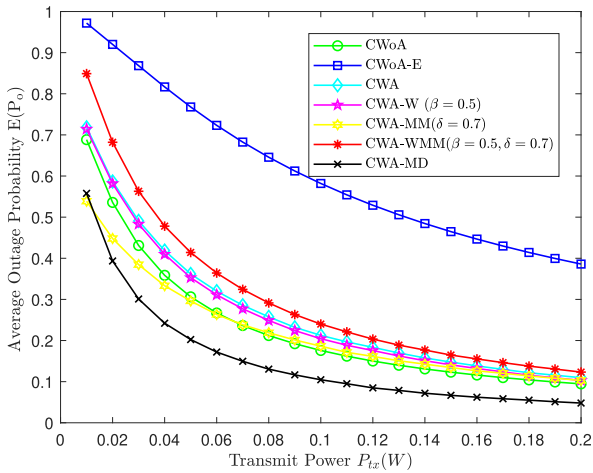


FIGURE 21. Average outage probability versus transmit power of UE's, $\beta = 0.5, \delta = 0.7$.

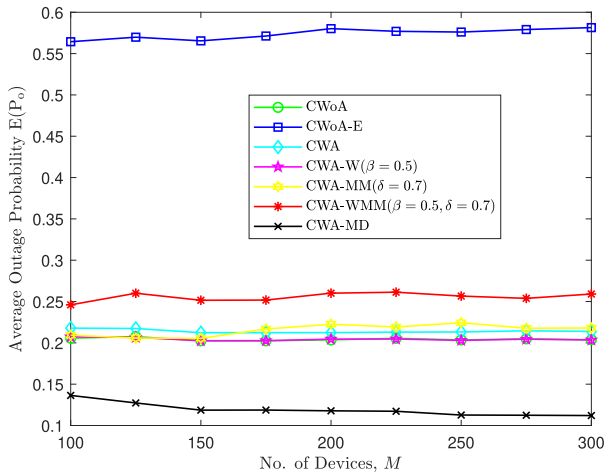


FIGURE 22. Average outage probability versus no of UE's without EH.

Fig. 23 shows the outage curves with HEH. The CWA and CWA-W schemes provide the best performance, whereas, the worst performing scheme depends on the basic transmit power. The outage curves saturate when the transmit power of UEs exceeds 0.14W. The CWA-MD, CWA, and CWA-W converge at higher values of transmit power. Unlike Fig. 22, the outage curves in Fig. 24 decrease with an increasing number of devices. This is mainly due to an increased number of clusters and subsequently more CHs with HEH.

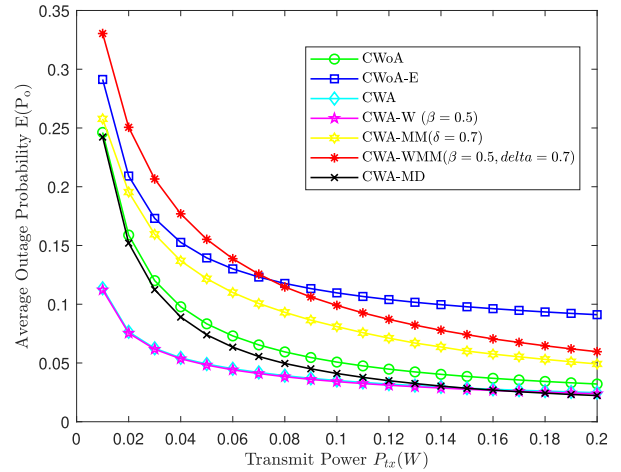


FIGURE 23. Average outage probability versus transmit power UE's with HEH, $\beta = 0.5, \delta = 0.7$.

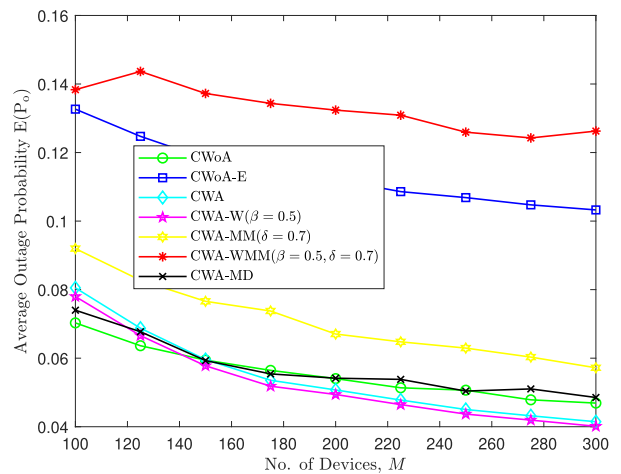


FIGURE 24. Average outage probability versus no of UE's with HEH, $\beta = 0.5, \delta = 0.7$.

V. CONCLUSION

In this paper, we present seven UAV assisted and disaster aware clustering schemes under different association metrics namely CWoA, CWoA-E, CWA, CWA-W, CWA-MD, CWA-MM, and CWA-WMM. The performance of these schemes is analyzed in terms of outage probability. Two scenarios were considered, 1) without SWIPT and 2) with SWIPT. Without SWIPT scenario CWA-MD provides the best outage performance, counter intuitively this is not the case in the SWIPT scenario. In all the SWIPT scenarios, CWA-W achieves lower outage by finding the best compromise between the intra-cluster distance and CH distance to the UAV. Restructuring of clusters in CWA-MM and CWA-WMM decreases the average number of hops at the cost of an increase in the average intra-cluster distance. The results show that this trade-off can be managed by using higher transmit power of the UEs. The above schemes are also applied to the layout of the real man-made disaster scenario of APS Peshawar in which the first responders could have benefited from the presence of MCC and UAV. The above observation regarding the clustering schemes remains equally valid despite a completely different layout of the UEs. In the future, we aim to

investigate the impact of UAV position and trajectory on the performance of proposed clustering schemes. The objective is to optimize the clustering specific parameters such as β and δ . In future, we also intend to explore non-linear energy harvesting model for more practical and realistic scenario.

REFERENCES

- [1] NDMA. *Pakistan 2005 Earthquake*. Accessed: Jun. 23, 2020. [Online]. Available: <https://bit.ly/3hPdLih>
- [2] NDMA. *Pakistan Floods 2010*. Accessed: May 10, 2020. [Online]. Available: <https://bit.ly/3hX6IUP>
- [3] Abbas. *Deciphering Attack Pakistan'S Army Headquarters*. Accessed: Jun. 20, 2020. [Online]. Available: <https://foreignpolicy.com/2009/10/11/deciphering-the-attack-on-pakistans-army-headquarters/>
- [4] CFD. *Disaster Philanthropy*. Accessed: Jun. 8, 2020. [Online]. Available: <https://disasterphilanthropy.org/our-approach/disasters/>
- [5] L. Babun, A. I. Yurekli, and I. Guvenc, "Multi-hop and D2D communications for extending coverage in public safety scenarios," in *Proc. IEEE 40th Local Comput. Netw. Conf. Workshops (LCN Workshops)*, Oct. 2015, pp. 912–919.
- [6] A. Masood, D. Scazzoli, N. Sharma, Y. L. Moullec, R. Ahmad, L. Reggiani, M. Magarini, and M. M. Alam, "Surveying pervasive public safety communication technologies in the context of terrorist attacks," *Phys. Commun.*, vol. 41, Aug. 2020, Art. no. 101109.
- [7] X. Zhou, S. Durrani, and J. Guo, "Drone-initiated D2D-aided multi-hop multicast networks for emergency information dissemination," *IEEE Access*, vol. 8, pp. 3566–3578, 2020.
- [8] H. I. Minhas, R. Ahmad, W. Ahmed, M. M. Alam, and M. Magarini, "On the impact of clustering for energy critical public safety networks," in *Proc. Int. Symp. Recent Adv. Electr. Eng. (RAEE)*, vol. 4, Aug. 2019, pp. 1–5.
- [9] M. Biabani, H. Fotouhi, and N. Yazdani, "An energy-efficient evolutionary clustering technique for disaster management in IoT networks," *Sensors*, vol. 20, no. 9, p. 2647, May 2020.
- [10] L. F. Del Carpio, A. A. Dowhuszko, O. Tirkkonen, and G. Wu, "Simple clustering methods for multi-hop cooperative Device-to-Device communication," in *Proc. IEEE 81st Veh. Technol. Conf. (VTC Spring)*, May 2015, pp. 1–6.
- [11] S. Shakoor, Z. Kaleem, M. I. Baig, O. Chughtai, T. Q. Duong, and L. D. Nguyen, "Role of UAVs in public safety communications: Energy efficiency perspective," *IEEE Access*, vol. 7, pp. 140665–140679, 2019.
- [12] L. D. Nguyen, K. K. Nguyen, A. Kortun, and T. Q. Duong, "Real-time deployment and resource allocation for distributed UAV systems in disaster relief," in *Proc. IEEE 20th Int. Workshop Signal Process. Adv. Wireless Commun. (SPAWC)*, Jul. 2019, pp. 1–5.
- [13] F. Chen, R. Chang, W. Lin, S. H. Chen, Y. C. Chen, and C. N. Li, "Disaster and Emergency Management System," in *Proc. 15th Int. Symp. Wireless Pers. Multimedia Commun.*, Sep. 2012, pp. 363–368.
- [14] V. Ponnusamy, Y. P. Tay, L. H. Lee, T. J. Low, and C. W. Zhao, "Energy harvesting methods for Internet of Things," in *Securing the Internet of Things: Concepts, Methodologies, Tools, and Applications*. Hershey, PA, USA: IGI Global, 2020, pp. 956–976.
- [15] M. Imran, L. U. Khan, I. Yaqoob, E. Ahmed, M. Ahsan Qureshi, and A. Ahmed, "Energy harvesting in 5G networks: Taxonomy, requirements, challenges, and future directions," 2019, *arXiv:1910.00785*. [Online]. Available: <http://arxiv.org/abs/1910.00785>
- [16] M. Wagih, A. S. Weddell, and S. Beeby, "Millimeter-wave textile antenna for on-body RF energy harvesting in future 5G networks," in *Proc. IEEE Wireless Power Transf. Conf. (WPTC)*, London, U.K., 2019, pp. 245–248, doi: [10.1109/WPTC45513.2019.9055541](https://doi.org/10.1109/WPTC45513.2019.9055541).
- [17] W. Kruskamp, "From Bluetooth low-energy to Bluetooth no-energy: System and circuit aspects of energy harvesting for IoT applications," in *Low-Power Analog Techniques, Sensors for Mobile Devices, and Energy Efficient Amplifiers*. Cham, Switzerland: Springer, 2019, pp. 13–30, doi: [10.1007/978-3-319-97870-3_2](https://doi.org/10.1007/978-3-319-97870-3_2).
- [18] C. X. Mavromoustakis, G. Mastorakis, and J. M. Batalla, *Internet of Things (IoT) in 5G Mobile Technologies*, vol. 8. Cham, Switzerland: Springer, 2016, doi: [10.1007/978-3-319-30913-2](https://doi.org/10.1007/978-3-319-30913-2).
- [19] P. A. Owusu and S. Asumadu-Sarkodie, "A review of renewable energy sources, sustainability issues and climate change mitigation," *Cogent Eng.*, vol. 3, no. 1, Apr. 2016, Art. no. 1167990.
- [20] Y. Luo, L. Pu, G. Wang, and Y. Zhao, "RF energy harvesting wireless communications: RF environment, device hardware and practical issues," *Sensors*, vol. 19, no. 13, p. 3010, Jul. 2019.
- [21] R. Y. Chang, "D2D with energy harvesting capabilities," in *Wiley 5G Ref: The Essential 5G Reference Online*. Hoboken, NJ, USA: Wiley, 2019, pp. 1–20.
- [22] O. Assogba, A. K. Mbodji, and A. K. Diallo, "Efficiency in RF energy harvesting systems: A comprehensive review," in *Proc. IEEE Int. Conf. Natural Eng. Sci. Sahel's Sustain. Develop. Impact Big Data Appl. Soc. Environ. (IBASE-BF)*, Feb. 2020, pp. 1–10.
- [23] I. Krikidis, S. Timotheou, S. Nikolaou, G. Zheng, D. W. K. Ng, and R. Schober, "Simultaneous wireless information and power transfer in modern communication systems," *IEEE Commun. Mag.*, vol. 52, no. 11, pp. 104–110, Nov. 2014.
- [24] E. Boshkovska, D. W. K. Ng, N. Zlatanov, and R. Schober, "Practical non-linear energy harvesting model and resource allocation for SWIPT systems," *IEEE Commun. Lett.*, vol. 19, no. 12, pp. 2082–2085, Dec. 2015.
- [25] S. Yin, Y. Zhao, and L. Li, "UAV-assisted cooperative communications with time-sharing SWIPT," in *Proc. IEEE Int. Conf. Commun. (ICC)*, May 2018, pp. 1–6.
- [26] O. M. Bushnaq, A. Chaaban, and T. Y. Al-Naffouri, "The role of UAV-IoT networks in future wildfire detection," 2020, *arXiv:2007.14158*. [Online]. Available: <http://arxiv.org/abs/2007.14158>
- [27] K. Ali, H. X. Nguyen, Q.-T. Vien, P. Shah, and Z. Chu, "Disaster management using D2D communication with power transfer and clustering techniques," *IEEE Access*, vol. 6, pp. 14643–14654, 2018.
- [28] Z. Yang, C. Pan, M. Shikh-Bahaei, W. Xu, M. Chen, M. Elakashlan, and A. Nallanathan, "Joint altitude, beamwidth, location, and bandwidth optimization for UAV-enabled communications," *IEEE Commun. Lett.*, vol. 22, no. 8, pp. 1716–1719, Aug. 2018.
- [29] F. Mezghani and N. Mitton, "Opportunistic multi-technology cooperative scheme and UAV relaying for network disaster recovery," *Information*, vol. 11, no. 1, p. 37, Jan. 2020.
- [30] Y. Xu and B. Liu, "Disaster-recovery communications utilizing SWIPT-based D2D relay network," in *Proc. IEEE 5th Int. Conf. Comput. Commun. (ICCC)*, Dec. 2019, pp. 1041–1046.
- [31] D. N. K. Jayakody, T. D. P. Perera, A. Ghayeb, and M. O. Hasna, "Self-energyized UAV-assisted scheme for cooperative wireless relay networks," *IEEE Trans. Veh. Technol.*, vol. 69, no. 1, pp. 578–592, Jan. 2020.
- [32] N. Zhao, W. Lu, M. Sheng, Y. Chen, J. Tang, F. R. Yu, and K.-K. Wong, "UAV-assisted emergency networks in disasters," *IEEE Wireless Commun.*, vol. 26, no. 1, pp. 45–51, Feb. 2019.
- [33] Z. Yang, W. Xu, and M. Shikh-Bahaei, "Energy efficient UAV communication with energy harvesting," *IEEE Trans. Veh. Technol.*, vol. 69, no. 2, pp. 1913–1927, Feb. 2020.
- [34] Z. Zhu, Z. Chu, F. Zhou, H. Niu, Z. Wang, and I. Lee, "Secure beamforming designs for secrecy MIMO SWIPT systems," *IEEE Wireless Commun. Lett.*, vol. 7, no. 3, pp. 424–427, Jun. 2018.
- [35] Z. Zhu, S. Huang, Z. Chu, F. Zhou, D. Zhang, and I. Lee, "Robust designs of beamforming and power splitting for distributed antenna systems with wireless energy harvesting," *IEEE Syst. J.*, vol. 13, no. 1, pp. 30–41, Mar. 2019.
- [36] W. Wang, X. Li, M. Zhang, K. Cumanan, D. W. Kwan Ng, G. Zhang, J. Tang, and O. A. Dobre, "Energy-constrained UAV-assisted secure communications with position optimization and cooperative jamming," *IEEE Trans. Commun.*, vol. 68, no. 7, pp. 4476–4489, Jul. 2020.
- [37] Z. Chu, F. Zhou, P. Xiao, Z. Zhu, D. Mi, N. Al-Dhahir, and R. Tafazolli, "Resource allocation for secure wireless powered integrated multicast and unicast services with full duplex self-energy recycling," *IEEE Trans. Wireless Commun.*, vol. 18, no. 1, pp. 620–636, Jan. 2019.
- [38] D. W. K. Ng, E. S. Lo, and R. Schober, "Robust beamforming for secure communication in systems with wireless information and power transfer," *IEEE Trans. Wireless Commun.*, vol. 13, no. 8, pp. 4599–4615, Aug. 2014.
- [39] Z. Chu, Z. Zhu, M. Johnston, and S. Y. Le Goff, "Simultaneous wireless information power transfer for MISO secrecy channel," *IEEE Trans. Veh. Technol.*, vol. 65, no. 9, pp. 6913–6925, Sep. 2016.
- [40] S. Ghosh, S. Mondal, S. D. Roy, and S. Kundu, "D2D communication with energy harvesting relays for disaster management," *Int. J. Electron.*, vol. 107-2020, no. 8, pp. 1–19, 2020, doi: [10.1080/00207217.2020.1726488](https://doi.org/10.1080/00207217.2020.1726488).
- [41] E. Ever, E. Gemikonakli, H. X. Nguyen, F. Al-Turjman, and A. Yazici, "Performance evaluation of hybrid disaster recovery framework with D2D communications," *Comput. Commun.*, vol. 152, pp. 81–92, Feb. 2020.
- [42] S. Ahmed, M. Rashid, F. Alam, and B. Fakhruddin, "A disaster response framework based on IoT and D2D communication under 5G network technology," in *Proc. 29th Int. Telecommun. Netw. Appl. Conf. (ITNAC)*, Nov. 2019, pp. 1–6.

- [43] U. N. Kar and D. K. Sanyal, "An overview of device-to-device communication in cellular networks," *ICT Express*, vol. 4, no. 4, pp. 203–208, Dec. 2018.
- [44] S. Abdellatif, O. Tibermacine, W. Bechkit, and A. Bachir, "Efficient distributed D2D ProSe-based service discovery and querying in disaster situations," in *Advanced Information Networking and Applications*, L. Barolli, F. Amato, F. Moscato, T. Enokido, and M. Takizawa, Eds. Cham, Switzerland: Springer, 2020, pp. 910–921.
- [45] A. Asadi and V. Mancuso, "WiFi direct and LTE D2D in action," in *Proc. IFIP Wireless Days (WD)*, Nov. 2013, pp. 1–8.
- [46] L. Yang, J. Chen, M. O. Hasna, and H.-C. Yang, "Outage performance of UAV-assisted relaying systems with RF energy harvesting," *IEEE Commun. Lett.*, vol. 22, no. 12, pp. 2471–2474, Dec. 2018.
- [47] BBC. *Peshawar School Massacre: What We Know*. Accessed: Jun. 13, 2020. [Online]. Available: <https://www.bbc.com/news/world-asia-30488503>



ALI HASSAN received the B.S. degree in electrical engineering (telecommunication and electronics) from The University of Lahore, Pakistan, in 2018, and the M.Sc. degree in electrical engineering (telecommunication and networks) from the National University of Sciences and Technology, Pakistan. He received a certificate of excellence for achieving academic excellence in the B.Sc. degree in electrical engineering in the Session Fall 2014. He is currently working as a

Research Assistant with the School of Electrical Engineering and Computer Science, National University of Sciences and Technology, Pakistan. His research interests include software-defined networking, blockchain, energy harvesting, the Internet of Things, and public safety and critical networks. He is a Research Assistant of NATO-SPS-G5482.



RIZWAN AHMAD (Member, IEEE) received the M.Sc. degree in communication engineering and media technology from the University of Stuttgart, Stuttgart, Germany, in 2004, and the Ph.D. degree in electrical engineering from Victoria University, Melbourne, Australia, in 2010. From 2010 to 2012, he was a Postdoctoral Research Fellow with Qatar University on a QNRF Grant. He is currently an Assistant Professor with the School of Electrical Engineering and Computer Science, National University of Sciences and Technology, Pakistan. He has published and served

as a reviewer for the IEEE journals and conferences. His research interests include medium access control protocols, spectrum and energy efficiency, energy harvesting, and performance analysis for wireless communication and networks. He also serves on the TPC of leading conferences in the communication and networking field, i.e., the IEEE VTC, IEEE ICC, and IEEE Globecom. He was a recipient of the prestigious International Postgraduate Research Scholarship from the Australian Government.



WAQAS AHMED (Member, IEEE) received the M.S. degree in systems engineering from the Pakistan Institute of Engineering and Applied Sciences, in 2005, and the Ph.D. degree in electrical engineering from Victoria University, Melbourne, Australia, in 2012. Since 2007, he has been an Assistant Professor with the Department of Electrical Engineering, Pakistan Institute of Engineering and Applied Sciences. His research interests include cognitive radios, cooperative communication, and physical layer aspects of wireless communication and networks.

He has published and served as a reviewer for the IEEE journals and conferences. He also serves on the TPC of leading conferences in the communication and networking field, i.e., the IEEE VTC, IEEE ICC, and IEEE WCNC. He was a recipient of the IEEE Exemplary Reviewer Award, in 2010.



MAURIZIO MAGARINI (Member, IEEE) received the M.Sc. and Ph.D. degrees in electronic engineering from the Politecnico di Milano, Milan, Italy, in 1994 and 1999, respectively. In 1994, he was granted the TELECOM Italia Scholarship Award for his M.Sc. Thesis. He worked as a Research Associate with the Dipartimento di Elettronica, Informazione e Bioingegneria, Politecnico di Milano, from 1999 to 2001. From 2001 to 2018, he was an Assistant Professor with the Politecnico di Milano, where he has been an Associate Professor since June 2018. From August 2008 to January 2009, he spent a sabbatical leave at Bell Labs, Alcatel-Lucent, Holmdel, NJ, USA. His research interests are in the broad area of communication and information theory. His research topics include synchronization, channel estimation, equalization and coding applied to wireless and optical communication systems. His most recent research activities have focused on molecular communications, massive MIMO, the study of waveforms for 5G cellular systems, wireless sensor networks for mission-critical applications, and wireless networks using UAVs and high-altitude platforms. He has authored and coauthored more than 100 journal and conference papers. He was a co-recipient of four best paper awards. Since 2017, he has been an Associate Editor of IEEE Access and a member of the Editorial Board of *Nano Communication Networks* (Elsevier). In 2017, he also served as a Guest Editor for the IEEE Access Special Section on "Networks of Unmanned Aerial Vehicles: Wireless Communications, Applications, Control and Modelling." He has been involved in several European and National research projects.



MUHAMMAD MAHTAB ALAM (Senior Member, IEEE) received the M.Sc. degree in electrical engineering from Aalborg University, Denmark, in 2007, and the Ph.D. degree in signal processing and telecommunication from the University of Rennes1 France (INRIA Research Center), in 2013. He joined the Swedish College of Engineering and Technology, Pakistan, in 2013, as an Assistant Professor. He did his postdoctoral research (2014–2016) at the Qatar Mobility Innovation Center, Qatar. In 2016, he joined as the European Research Area Chair and as an Associate Professor with the Thomas Johann Seebeck Department of Electronics, Tallinn University of Technology, where he was elected as a Professor in 2018. Since 2019, he has been the Communication Systems Research Group Leader. His research focuses on the fields of wireless communications—connectivity, NB-IoT 5G/B5G services and applications, as well as low-power wearable networks for SmartHealth.

He has over 15 years of combined academic and industrial multinational experiences while working in Denmark, Belgium, France, Qatar, and Estonia. He has several leading roles as PI in multimillion Euros international projects funded by European Commission (H2020-ICT-2019-3, "951867", NATOSPS (G5482), Estonian Research Council (PRG424), Telia Industrial Grant. He is an author and co-author of more than 80 research publications. He is actively supervising a number of Ph.D. and Postdoc Researchers. He is also a contributor in two standardization bodies (ETSI SmartBAN, IEEE-GeenICT-EECH), including "Rapporteur" of work item: DTR/SmartBAN-0014, "Applying SmartBAN MAC (TS 103 325) for various use cases." He is an Associate Editor of IEEE Access.

...